The phase diagram of QCD from lattice simulations

Massimo D'Elia

Dipartimento di Fisica dell'Università di Pisa
and INFN - Sezione di Pisa, Largo Pontecorvo 3, I-56127 Pisa, Italy

Numerical simulations of Quantum Chromodynamics on a space-time lattice represent the best non-perturbative tool to explore the QCD phase diagram and the behavior of strong interactions under extreme conditions. We review the present status of the field and discuss some recent results.

1. Introduction

Many of the questions which are still open within the Standard Model of particle physics concern strong interactions. They are described by Quantum Chromodynamics (QCD). While we have a clear understanding of the theory in the high energy limit where, thanks to property of asymptotic freedom, it is perturbative, we still cannot solve the low energy regime, where the coupling is strong and the theory is non-perturbative. As a result, we still do not understand why quarks and gluons, the elementary colored degrees of freedom of QCD, are confined into hadrons. One would also like to know if color confinement is a permanent state of matter, or if in particular extreme conditions, characterized by high temperature, high baryon density or strong magnetic fields, different phases of strongly interacting matter can be found.

The possible presence of a high temperature deconfined Quark-Gluon plasma phase has been explored since long: it is of particular interest for cosmological and astrophysical reasons (think, e.g., of the early stages of evolution of the Universe), and it is experimentally probed by heavy ion collision experiments.

Numerical simulations of QCD discretized on a Euclidean space-time lattice represent the best available tool to explore strong interactions in the non-perturbative regime, starting from the first principles of the theory. In practice, one rewrites the QCD thermal partition function, formulated in the Feynman path integral formalism, as follows

$$Z(V,T) = \int \mathcal{D}U\mathcal{D}\psi\mathcal{D}\bar{\psi} e^{-(S_G[U]+\bar{\psi}M[U]\psi)} = \int \mathcal{D}U e^{-S_G[U]} \det M[U] \, ,$$

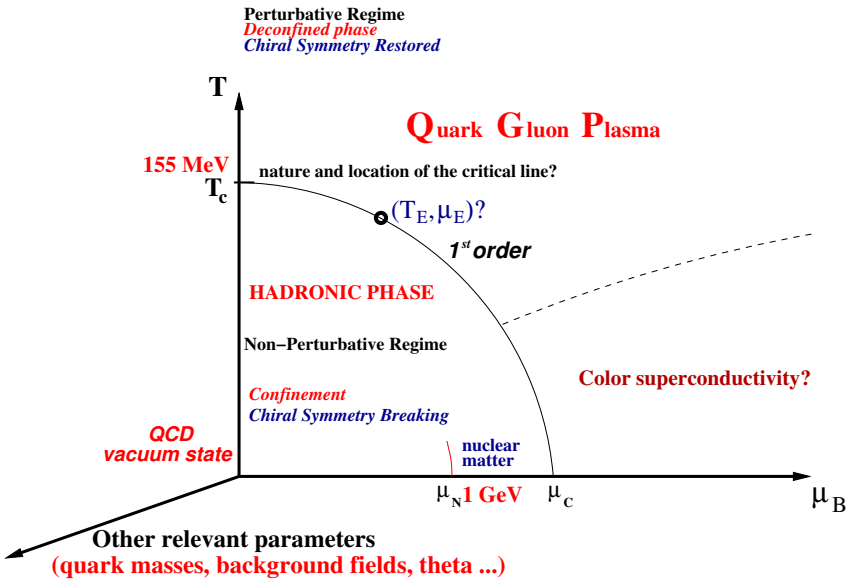

Fig. 1. Schematic view of the QCD phase diagram. The $T - \mu_B$ plane is shown in more detail, together with some questions that lattice simulations still leave open.

where U are the gauge link variables (elementary parallel transports) and $\bar{\psi} M \psi$ is a proper discretization of the quark action. The temperature T is related to the extension of the compactified Euclidean time dimension τ, $T = 1/\tau = 1/(N_t a)$ where a is the lattice spacing (we assume an isotropic cubic lattice) and N_t is the number of lattice sites in the time direction. $S_G[U]$ is the pure gauge action while $\det M$ encodes the contribution of dynamical fermions. Lattice simulations are ideally suited to compute equilibrium quantities, like

$$\langle O \rangle_T = \frac{\int \mathcal{D}U e^{-S_G[U]} \det M[U] O[U]}{\int \mathcal{D}U e^{-S_G[U]} \det M[U]} = \int \mathcal{D}U \mathcal{P}[U] O[U] \, ,$$

where O is a generic physical observable, via Monte-Carlo sampling. An obvious requirement is that the probability distribution over gauge configurations, $\mathcal{P}[U]$, be real and positive. In general, the correct inclusion of the fermion determinant in the probability distribution is the most demanding task in terms of computational power, especially when one tries to lower the values of the light quark masses towards their physical values.

Lattice simulations give us information, with a systematically increasable precision, about basic thermodynamical quantities, like the pressure and the

energy density, about equilibrium particle and quantum number distributions (e.g., quadratic and higher order susceptibilities of baryon number and electric charge) and on the location and the order of the transitions to the different phases of strongly interacting matter, i.e. about the QCD phase diagram, which is reported schematically in Fig. 1. Apart from temperature, one can think of many possible extensions of the phase diagram, representing external parameters of phenomenological relevance. Unfortunately, the important case of a baryonic chemical potential μ_B, which is necessary to consider QCD at finite density, is plagued by the so-called sign problem: the fermion determinant $\det M[\mu_B \neq 0]$ is complex, so that the path integral measure is not positive and Monte-Carlo methods are not directly usable. Approximate methods works well only in a limited region where $\mu_B/T \ll 1$, which is the case of the strongly interacting medium produced in heavy ion collisions at very high energies ($\mu_B/T \sim 10^{-2}$ at LHC).

2. Phase diagram at zero and non-zero baryon density

The liberation of color degrees of freedom at the deconfinement temperature is clearly visible, in lattice studies, from the sudden increase of approximate order parameters, like the Polyakov loop, and of various thermodynamical quantities, like the energy density, the pressure or the quark number susceptibilities. Roughly around the same temperature, the restoration of chiral symmetry, which is spontaneously broken at low T, takes place. There is now good agreement between different collaborations, adopting different discretizations schemes, regarding the location of this transition, which according to chiral symmetry restoration is placed around $T_c \sim 155$ MeV [1, 2].

The behavior of various susceptibilities is consistent with the absence of a true transition, i.e. no discontinuities seem to develop as the thermodynamical limit is approached [3]: that means that either the transition is extremely weak (hence not phenomenologically relevant) or deconfinement and chiral symmetry restoration correspond simply to a rapid change of physical properties.

Actually, this is the situation for physical values of the quark masses. In numerical simulations the quark mass spectrum can be changed at will and one can explore the nature of the transition as a function of u/d and s quark masses. The present outcome of such exploration is reported in Fig. 2, which is usually known as the Columbia plot. A true transition is present in the limit of very light or very heavy quark masses, where exact symmetries and order parameters can be found (chiral and center symmetry respectively). Unsettled issues exist regarding the chiral limit of the two flavor theory [4], where the transition could be first order or second order

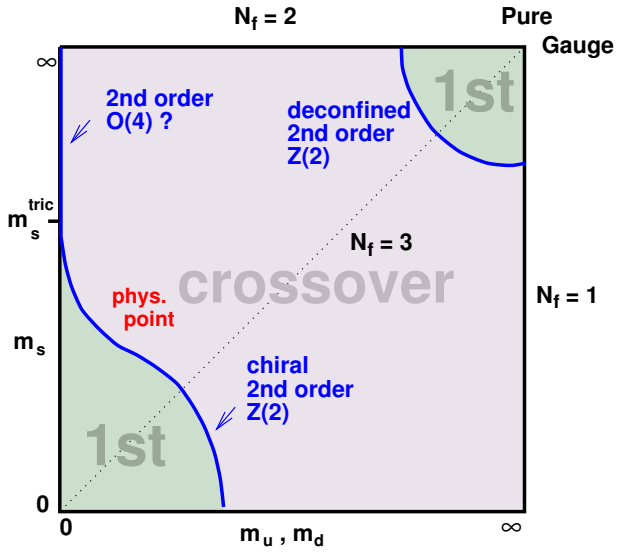

Fig. 2. Phase structure of $N_f = 2 + 1$ QCD as a function of the up/down and strange quark masses.

in the $O(4)$ universality class.

When one considers the various possible extensions of the phase diagram, like the inclusion of a baryon chemical potential μ_B, one would like to determine how T_c changes and if it corresponds to a true transition at some stage, for instance at a critical endpoint in the $T - \mu_B$ plane. For QCD at finite baryon density reliable numerical results can be obtained only in a restricted region of high T and small chemical potentials, where approximate solutions to the sign problem can be found, like reweighting techniques [5, 6], analytic continuation from imaginary chemical potentials [7–9] and Taylor expansion techniques [10, 11].

As an example, in Fig. 2 we report a comparison (see Ref. [12]) of the critical line $T_c(\mu_B)$ determined in the case of four degenerate flavors by different techniques (the pseudocritical temperature T_c is an increasing function of the pseudocritical coupling β_c, which is the quantity reported in the figure). Consistency among different determinations is good as long $\mu/T \leq 1$ (μ is the quark chemical potential, i.e. $\mu \equiv \mu_B/3$), meaning that the curvature of the pseudocritical line at $\mu = 0$ can be determined with good control over systematic uncertainties. In the physical case of 2 or 2+1 flavors one obtains values for the curvature of the critical line, $T_c(\mu)/T_c(0) = 1 - A\,(\mu/T)^2$, in the range $A \sim 0.05 - 0.07$ [8, 13–15]. Such values are smaller, by ap-

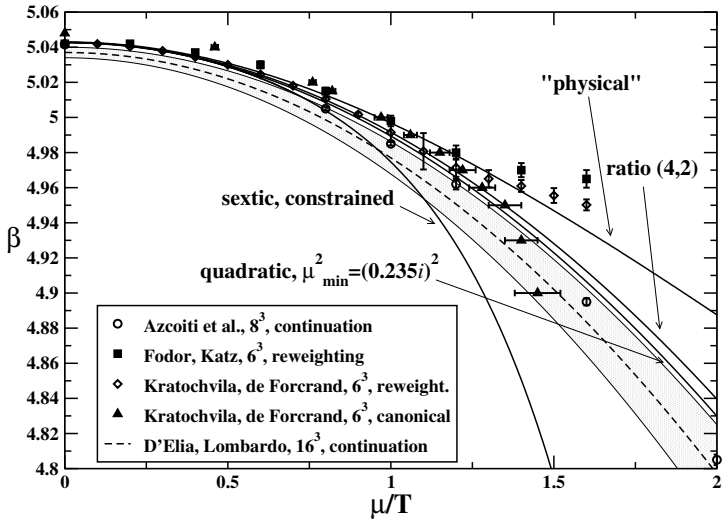

Fig. 3. Determination of the line of pseudo-critical couplings for deconfinement as a function of the quark chemical potential μ for $N_f = 4$ QCD. Various different methods are compared, including different extrapolations from simulations at imaginary chemical potentials.

proximately a factor 3, than those usually obtained for chemical freeze-out curves in heavy ion collisions. However a recent re-analysis of heavy-ion data, which takes better into account inelastic interactions after hadronization, seems to bring the freeze-out curves closer to lattice predictions for the pseudocritical line [16, 17].

Unfortunately the same techniques, working well for small baryon chemical potentials, have not provided, up to now, a clear and consistent evidence for the presence and the location of the critical endpoint in the $T-\mu_B$ plane, at which the pseudo-transition present at $\mu_B = 0$ would turn into a first order transition.

The general idea is that the introduction of non-zero μ_B would increase the strength of the transition, thus enlarging the low-mass first order region in Fig. 2 till the physical point is included into it. However, numerical simulations performed at imaginary chemical potential, i.e. negative μ_B^2, seem indicate that the effect of a a positive μ_B^2 is instead to decrease the strength of the transition [18]. This has been recently reinterpreted in terms of the general structure of the phase diagram at $\mu_B^2 < 0$, in particular in connection with the phase structure close to the so-called Roberge-Weiss endpoint [19, 20] and the related tricritical points. In Fig. 2 we show the

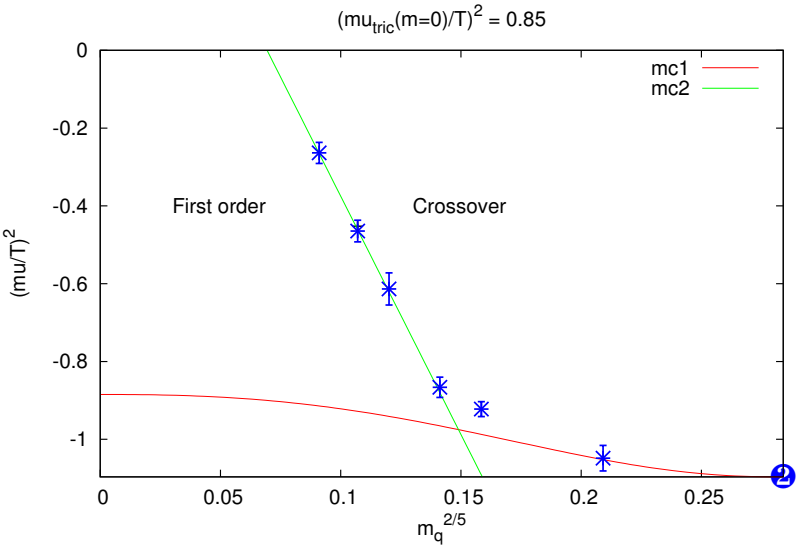

Fig. 4. Phase structure of $N_f = 2$ QCD in the bare quark mass - imaginary chemical potential plane. Imaginary chemical potentials correspond negative values of μ^2. The scale chosen for the quark mass axis permits to better appreciate the chiral extrapolation according to tricritical scaling (see Ref. [21]).

result of recent extensive studies regarding the order of the phase transition for the theory with two light flavors, $N_f = 2$ QCD, as a function of the bare quark mass and μ^2 [21]: the first order region clearly shrinks as μ^2 increases; moreover, present results suggest that the chiral limit at $\mu = 0$, i.e. the left-upper corner in Fig. 2, might be first order, in agreement also with the findings of Ref. [4].

3. Strongly interacting matter in strong magnetic fields

Quarks are also subject to electromagnetic interactions, which however are expected, in general, to bring small corrections to strong interaction physics. Nevertheless, the situation may be different in the presence of background fields whose strenght is at the QCD scale. The issue is of great phenomenological interest, since in some heavy ion collisions one has the highest magnetic fields ever created in a laboratory [22], reaching up to 10^{15} Tesla ($eB \sim 0.1$ GeV^2) at LHC, and even larger fields may have been created in the early stages of the Universe [23, 24].

That justifies the recent theoretical interest in the subject [25]. Contrary

to the case of a finite μ_B, the introduction of a magnetic background field does not encounter particular technical problems, such as a sign problem, so that various interesting questions can be conveniently approached and have been investigated by lattice QCD simulations in the last few years [26–43].

Lattice results show that T_c decreases as a function of the external field, with deconfinement and chiral symmetry breaking remaining entangled. The strength of the transition increases, in the sense that the rapid change of thermodynamical quantities becomes steeper and steeper, even if no evidence has been found till now for a critical endpoint in the $T - B$ plane where T_c becomes a true transition point.

Various studies have investigated the magnetic properties of strongly interacting matter. The outcome is that it behaves as a paramagnetic material [38–40, 43], with a magnetic susceptibility which steeply rises as one enters the deconfined Quark-Gluon Plasma phase, and is comparable to that of well known strong paramagnetic materials, such as liquid oxygen.

References

[1] S. Borsanyi *et al.*, J. High Energy Phys. **09**, 073 (2010).
[2] A. Bazavov *et al.*, Phys. Rev. D, **85**, 054503 (2012).
[3] Y. Aoki, Z. Fodor, S.D. Katz, and K. K. Szabo, Phys. Lett. B **643**, 46 (2006).
[4] M. D'Elia, A. Di Giacomo, and C. Pica, Phys. Rev. D **72**, 114510 (2005); G. Cossu, M. D'Elia, A. Di Giacomo, and C. Pica, arXiv:0706.4470 [hep-lat].
[5] I.M. Barbour *et al.*, Nucl. Phys. (Proc. Suppl.) A **60**, 220 (1998).
[6] Z. Fodor and S.D. Katz, Phys. Lett. B **534**, 87 (2002).
[7] M.G. Alford, A. Kapustin, and F. Wilczek, Phys. Rev. D **59**, 054502 (1999).
[8] P. de Forcrand and O. Philipsen, Nucl. Phys. B **642**, 290 (2002).
[9] M. D'Elia and M.P. Lombardo, Phys. Rev. D **67**, 014505 (2003).
[10] C.R. Allton *et al.*, Phys. Rev. D **66**, 074507 (2002).
[11] R.V. Gavai and S. Gupta, Phys. Rev. D **68**, 034506 (2003).
[12] P. Cea, L. Cosmai, M. D'Elia, and A. Papa, Phys. Rev. D **81**, 094502 (2010).
[13] O. Kaczmarek *et al.*, Phys. Rev. D **83**, 014504 (2011).
[14] G. Endrodi, Z. Fodor, S.D. Katz, and K.K. Szabo, J. High Energy Phys. **04**, 001 (2011).
[15] P. Cea *et al.*, Phys. Rev. D, **85**, 094512 (2012).
[16] F. Becattini *et al.*, Phys. Rev. C **85**, 044921 (2012).
[17] F. Becattini *et al.*, Phys. Rev. Lett. **111**, 082302 (2013).

[18] P. de Forcrand and O. Philipsen, J. High Energy Phys. **01**, 077 (2007); J. High Energy Phys. **11**, 012 (2008).
[19] A. Roberge and N. Weiss, Nucl. Phys. B **275**, 734 (1986).
[20] M. D'Elia and F. Sanfilippo, Phys. Rev. D **80**, 111501 (2009); P. de Forcrand and O. Philipsen, Phys. Rev. Lett. **105**, 152001 (2010); C. Bonati, G. Cossu, M. D'Elia, and F. Sanfilippo, Phys. Rev. D **83**, 054505 (2011).
[21] C. Bonati *et al.*, PoS LATTICE **2011**, 189 (2011); arXiv:1311.0473.
[22] V. Skokov, A.Y. .Illarionov and V. Toneev, Int. J. Mod. Phys. A **24**, 5925 (2009); V. Voronyuk *et al.*, Phys. Rev. C **83**, 054911 (2011); A. Bzdak and V. Skokov, W.-T. Deng and X.-G. Huang, Phys. Rev. C **85**, 044907 (2012).
[23] T. Vachaspati, Phys. Lett. B **265**, 258 (1991).
[24] D. Grasso and H.R. Rubinstein, Phys. Rept. **348**, 163 (2001).
[25] D. Kharzeev, K. Landsteiner, A. Schmitt, and H.-U. Yee, Lect. Notes Phys. **871**, 1 (2013).
[26] P. Cea and L. Cosmai, J. High Energy Phys. **08**, 079 (2005); P. Cea, L. Cosmai, and M. D'Elia, J. High Energy Phys. **12**, 097 (2007).
[27] P.V. Buividovich, M.N. Chernodub, E.V. Luschevskaya, and M.I. Polikarpov, Nucl. Phys. B **826**, 313 (2010).
[28] P.V. Buividovich, M.N. Chernodub, E.V. Luschevskaya, and M.I. Polikarpov, Phys. Rev. D **80**, 054503 (2009).
[29] M. Abramczyk, T. Blum, G. Petropoulos, and R. Zhou, PoS LAT **2009**, 181 (2009).
[30] P.V. Buividovich *et al.*, Phys. Rev. Lett. **105**, 132001 (2010).
[31] M. D'Elia, S. Mukherjee, F. Sanfilippo, Phys. Rev. D **82**, 051501 (2010).
[32] M. D'Elia and F. Negro, Phys. Rev. D **83**, 114028 (2011).
[33] V.V. Braguta *et al.*, Phys. Lett. B **718**, 667 (2012).
[34] E.-M. Ilgenfritz *et al.*, Phys. Rev. D **85**, 114504 (2012).
[35] G.S. Bali *et al.*, J. High Energy Phys. **02**, 044 (2012).
[36] G.S. Bali *et al.*, Phys. Rev. D **86**, 094512 (2012).
[37] G.S. Bali *et al.*, J. High Energy Phys. **04**, 130 (2013).
[38] C. Bonati *et al.*, Phys. Rev. Lett. **111**, 182001 (2013).
[39] C. Bonati *et al.*, arXiv:1310.8656 [hep-lat].
[40] L. Levkova and C. DeTar, arXiv:1309.1142 [hep-lat].
[41] M. D'Elia, M. Mariti, and F. Negro, Phys. Rev. Lett. **110**, 082002 (2013).
[42] E.-M. Ilgenfritz, M. Muller-Preussker, B. Petersson, and A. Schreiber, arXiv:1310.7876 [hep-lat].
[43] G.S. Bali, F. Bruckmann, G. Endrodi, and A. Schafer, arXiv:1310.8145 [hep-lat]; arXiv:1311.2559 [hep-lat].